Supporting Information

General Methods.

^{1}H NMR (400 MHz), and ^{31}P{^{1}H} NMR (162 MHz) spectra were recorded on a JEOL ECS-400 spectrometer in suitable solvent, and spectra were referenced to residual solvent (^{1}H) or external standard (^{31}P{^{1}H}: H_3PO_4). Magnetic susceptibility was measured in CD_2Cl_2 using the Evans method[S1] Evolved dihydrogen was quantified by a gas chromatography using a Shimadzu GC-8A with a TCD detector and a SHINCARBON ST (6 m × 3 mm). Elemental analyses were performed at Microanalytical Center of The University of Tokyo.

All manipulations were carried out under an atmosphere of nitrogen by using standard Schlenk techniques or glovebox techniques unless otherwise stated. Toluene was distilled from dark-blue Na/benzophenone ketyl solution, degassed, and stored over molecular sieves 4Å in a nitrogen-filled glove box. Other solvents were dried by general methods, and degassed before use. $C_5NH_3(CH_2P\textit{t}\text{-}Bu_2)_2$ (H-PNP$^{t\text{-Bu}}$, **1a**),[S2] $C_5NH_3(CH_2PAd_2)_2$ (H-PNP$^{\mathrm{Ad}}$, **1b**),[S3] $C_5NH_3(CH_2P\textit{i}\text{-}Pr)_2$ (H-PNP$^{i\text{-Pr}}$, **1c**),[S4] $C_5NH_3(CH_2PPh_2)_2$ (H-PNP$^{\mathrm{Ph}}$, **1d**),[S5] 4Ph-$C_5NH_2(CH_2P\textit{t}\text{-}Bu_2)_2$ (Ph-PNP$^{t\text{-Bu}}$, **1e**),[S6] 4Me-$C_5NH_2(CH_2P\textit{t}\text{-}Bu_2)_2$ (Me-PNP$^{t\text{-Bu}}$, **1f**),[S6] 4MeO-$C_5NH_2(CH_2P\textit{t}\text{-}Bu_2)_2$ (MeO-PNP$^{t\text{-Bu}}$, **1g**),[S6] 4Fc-$C_5NH_2(CH_2P\textit{t}\text{-}Bu_2)_2$ (Fc-PNP$^{t\text{-Bu}}$, **1h**),[S7] 4Rc-$C_5NH_2(CH_2P\textit{t}\text{-}Bu_2)_2$ (Rc-PNP$^{t\text{-Bu}}$, **1i**),[S7] , [$MoCl_3$(thf)$_3$],[S8] [MoI_3(thf)$_3$],[S9] [MoI_3(H-PNP$^{t\text{-Bu}}$)] (**2a**),[S10] [ColH]OTf (Col = 2,4,6-trimethylpyridine),[S11] CoCp$^*_2$ (Cp* = η^5-C_5Me_5)[S12] and KC_8[S13] were prepared according to the literature methods. Other reagents were purchased commercially and used as received.

Preparation of [MoI_3(R-PNP$^{R'}$)] (2b – 2i)

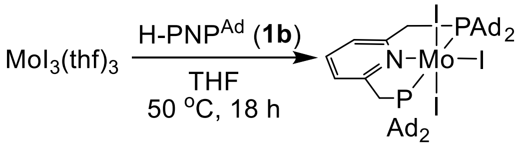

2b

A typical procedure for the preparation of [MoI_3(H-PNP$^{\mathrm{Ad}}$)] (**2b**) was described below. A mixture of [MoI_3(thf)$_3$] (34.6 mg, 0.0499 mmol) and **1b** (38.9 mg, 0.0549 mmol) in THF (3 mL) was stirred at 50 °C for 18 h. The resultant reddish-brown solution was filtered through Celite, and the filter cake was washed with THF (2 mL x 5). The combined filtrate was concentrated in vacuo, and the residue was washed with Et_2O (1 mL x 3) to afford **2b** as a brown solid (10.8 mg, 0.0912 mmol, 18% yield). In the synthesis of other complexes (**2c**-**2i**), recrystallization was carried out at this stage to obtain pure products. Unfortunately, we did not measure magnetic susceptibility of complex **2b** by Evans method due to the instability in the solution. Anal. Calcd. for $C_{47}H_{67}I_3MoNP_2$: C, 47.65; H, 5.70; N, 1.18. Found: C, 47.33; H, 5.33; N, 1.26.

[MoI_3(H-PNP$^{i\text{-Pr}}$)] (2c)

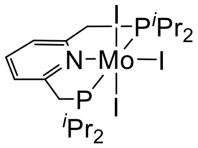

2c

Recrystallization from CH_2Cl_2-hexane gave orange crystals in 55% yield. Magnetic susceptibility (Evans method): μ_{eff} = 3.3 μ_{B} in CD_2Cl_2 at 294 K. Anal. Calcd. for $C_{19}H_{35}I_3MoNP_2$: C, 27.96; H, 4.32; N, 1.72. Found: C, 27.89; H, 4.22; N, 1.88.

[MoI_3(H-PNP^{Ph})] (2d)

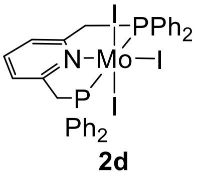

2d

Recrystallization from CH_2Cl_2-hexane gave red crystals in 30% yield. Magnetic susceptibility (Evans method): μ_{eff} = 3.9 μ_{B} in CD_2Cl_2 at 294 K. Anal. Calcd. for $C_{31}H_{27}I_3MoNP_2$: C, 39.10; H, 2.86; N, 1.47. Found: C, 38.84; H, 2.62; N, 1.52.

[MoI_3(Ph-PNP$^{t\text{-}Bu}$)] (2e)

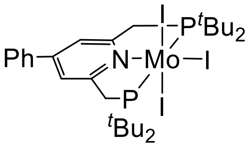

2e

Recrystallization from THF gave red crystals in 25% yield. Magnetic susceptibility (Evans method): μ_{eff} = 3.3 μ_{B} in CD_2Cl_2 at 294 K. Anal. Calcd. for $C_{29}H_{47}I_3MoNP_2$: C, 36.73; H, 5.00; N, 1.48. Found: C, 36.90; H, 4.77; N, 1.65.

[MoI_3(Me-PNP$^{t\text{-}Bu}$)] (2f)

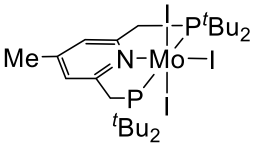

2f

Recrystallization from CH_2Cl_2-hexane gave dark red crystals in 55% yield. Magnetic susceptibility (Evans method): μ_{eff} = 3.5 μ_{B} in CD_2Cl_2 at 294 K. Anal. Calcd. for $C_{24}H_{45}I_3MoNP_2$: C, 32.53; H, 5.12; N, 1.58. Found: C, 32.84; H, 4.83; N, 1.46.

[MoI_3(MeO-PNP$^{t\text{-}Bu}$)] (2g)

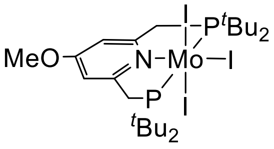

2g

Recrystallization from THF-Et_2O gave brown crystals in 40% yield. Magnetic susceptibility (Evans method): μ_{eff} = 3.5 μ_{B} in CD_2Cl_2 at 294 K. Anal. Calcd. for $C_{29}H_{47}I_3MoNOP_2$: C, 31.95; H, 5.03; N, 1.55. Found: C, 31.80; H, 4.80; N, 1.86.

[MoI$_3$(Fc-PNP$^{t\text{-Bu}}$)] (2h)

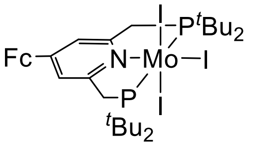

2h

Recrystallization from THF gave red purple crystals of **2h**·2THF in 62% yield. Magnetic susceptibility (Evans method): μ_{eff} = 3.5 μ_B in CD_2Cl_2 at 294 K. Anal. Calcd. for $C_{41}H_{67}FeI_3MoNO_2P_2$: C, 41.02; H, 5.63; N, 1.17. Found: C, 41.25; H, 5.65; N, 1.17.

[MoI$_3$(Rc-PNP$^{t\text{-Bu}}$)] (2i)

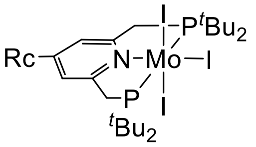

2i

Recrystallization from THF-Et_2O gave orange crystals of **2i**·2THF in 61% yield. Magnetic susceptibility (Evans method): μ_{eff} = 3.7 μ_B in CD_2Cl_2 at 294 K. Anal. Calcd. for $C_{41}H_{67}I_3MoNO_2P_2Ru$: C, 39.53; H, 5.42; N, 1.12. Found: C, 39.81; H, 5.14; N, 1.49.

Preparation of [Mo(N)I(Ph-PNP$^{t\text{-Bu}}$)] (3e).

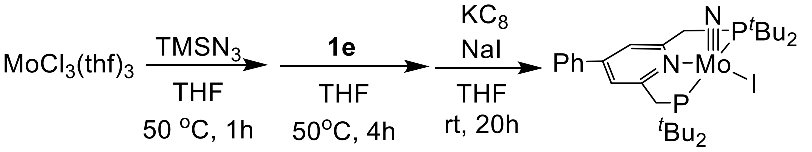

3e

A mixture of [$MoCl_3(thf)_3$] (120 mg, 0.287 mmol) and Me_3SiN_3 (40 µL, 0.304 mmol) in THF (6 mL) was stirred at 50 °C for 1 h. The resultant reddish brown solution was concentrated under reduced pressure. To the residue were added **1e** (140 mg, 0.297 mmol) and THF (30 mL), and then the mixture was stirred at 50 °C for 4 h. After cooling to room temperature, to the brown cloudy solution were added KC_8 (58.8 mg, 0.435 mmol) and NaI (290 mg, 1.93 mmol) and stirred at room temperature for 20 h. Volatiles were removed *in vacuo*, and benzene (10 mL) was added to the residue. The benzene solution was filtered through Celite, and the filter cake was washed with benzene (2 mL x 5). After the combined filtrate was concentrated to about 10 mL, slow addition of hexane (30 mL) afforded **3e** as brown crystals, which were collected by filtration, washed with hexane (1 mL x 3), and dried *in vacuo* (20.1 mg, 0.0284 mmol, 10% yield). $^{31}P\{^1H\}$ NMR (THF-d_8): 96.1 (s). ^1H NMR (THF-d_8): 8.00 (s, C_5H_2N, 2H), 7.83 (d, J = 3.6 Hz, ArH, 2H), 7.51-7.45 (m, ArH, 3H), 3.90 (br s, CH_2P, 4H), 1.58 (pseudo t, *J* = 6.8 Hz, P*t*-Bu$_2$, 18H), 1.26 (pseudo t, *J* = 6.8 Hz, P*t*-Bu$_2$, 18H). Anal. Calcd. for $C_{29}H_{47}IMoN_2P_2$: C, 49.16; H, 6.69; N, 3.95. Found: C, 48.78; H, 6.58; N, 4.04.

Preparation of [Mo(N)I(Fc-PNP$^{t\text{-Bu}}$)] (3h).

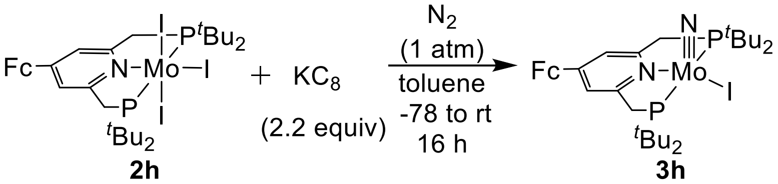

To a mixture of **2h**·2THF (120 mg, 0.100 mmol) and KC_8 (29.7 mg, 0.220 mmol) was added cooled toluene (20 mL, -78 °C) under N_2 (1 atm). After stirring at -78 °C for 5 min, the mixture was warmed to room temperature and further stirred at room temperature for 18 h. Volatiles were removed *in vacuo*, and washed with Et_2O (2 mL x 5). THF (5 mL) was added to the residue. The THF solution was filtered through Celite, and the filter cake was washed with THF (1 mL x 5). After the combined filtrate was concentrated to about 5 mL, slow addition of hexane (15 ml) afforded **3h**·THF as purple crystals, which were collected by filtration, washed with hexane (1 mL x 3), and dried *in vacuo* (21.6 mg, 0.0243 mmol, 24% yield. $^{31}P\{^1H\}$ NMR (THF-d_8): -. ^1H NMR (THF-d_8): 7.76 (s, C_5H_2N, 2H), 4.92 (br s, Cp*H*, 2H), 4.52 (br s, Cp*H*, 2H), 4.03 (s, Cp*H*, 5H), 3.81 (br s, CH_2P, 4H), 1.59 (pseudo t, *J* = 6.8 Hz, P*t*-Bu_2, 18H), 1.27 (pseudo t, *J* = 6.5 Hz, P*t*-Bu_2, 18H). Anal. Calcd. for $C_{37}H_{59}IMoN_2OP_2$: C, 50.01; H, 6.69; N, 3.15. Found: C, 50.06; H, 6.42; N, 3.08.

Catalytic reduction of dinitrogen into ammonia by molybdenum complexes. Typical experimental procedure.

In a nitrogen-filled glove box, to a mixture of **2a** (8.9 mg, 0.010 mmol) and [ColH]OTf (130 mg, 0.48 mmol) in a 50 mL Schlenk flask was added toluene (1 mL). Then a solution of $CoCp^*_2$ (118 mg, 0.36 mmol) in toluene (4 mL) was slowly added to the stirred suspension in the Schlenk flask with a syringe pump over a period of 1 h. After the addition of $CoCp^*_2$, the mixture was further stirred at room temperature for 19 h. The amount of molecular hydrogen of the catalytic reaction was determined by gas chromatography (GC). Potassium hydroxide aqueous solution (30 wt%; 5 mL) was added to the reaction mixture. The mixture was evaporated under reduced pressure, and the distillate was trapped in dilute H_2SO_4 solution (0.5 M, 10 mL). The amount of ammonia present in the H_2SO_4 solution was determined by the indophenol method.[S14] No hydrazine was detected by the *p*-(dimethylamino)benzaldehyde method.[S15]

Electrochemistry.

Cyclic voltammograms were recorded on an ALS/Chi model 610C electrochemical analyzer with platinum working electrode in THF containing 1 mM of sample and 0.1 M of [*n*-Bu_4N]BAr^F_4 (Ar^F = 3,5-$(CF_3)_2C_6H_3$) as supporting electrolyte at a scan rate of 0.1 V/s at room temperature. All potentials were measured against an $Ag^{0/+}$ electrode and converted to the values vs ferrocene/ferrocenium ($Fc^{0/+}$).

Time profiles of the formation of ammonia and molecular dihydrogen under slow addition conditions.

A typical procedure is as follows. In a 50 mL Schlenk flask were placed **2a** (0.002 mmol), [ColH]OTf (480 equiv/Mo), and toluene (1 mL) under N_2 (1 atm). A solution of $CoCp^*_2$ (360 equiv/Mo) in toluene (4 mL) was slowly added to the stirred mixture in the Schlenk flask with a syringe pump over a period of 1 h, and then the mixture was further stirred at room temperature for 19 h. After the indicated time (0.33 h, 0.66 h, 1 h, 2 h, and

20 h), the amount of molecular hydrogen in the catalytic reaction was determined by GC analysis, and then 30wt% potassium hydroxide aqueous solution (5 mL) was added to the reaction mixture. The mixture was evaporated under reduced pressure, and the distillate was trapped in dilute H_2SO_4 solution (0.5 M, 10 mL). The amount of ammonia present in the H_2SO_4 solution was determined by the indophenol method.[S14] The results are summarized in Figures S1 and S2 ,and Tables S1-S3.

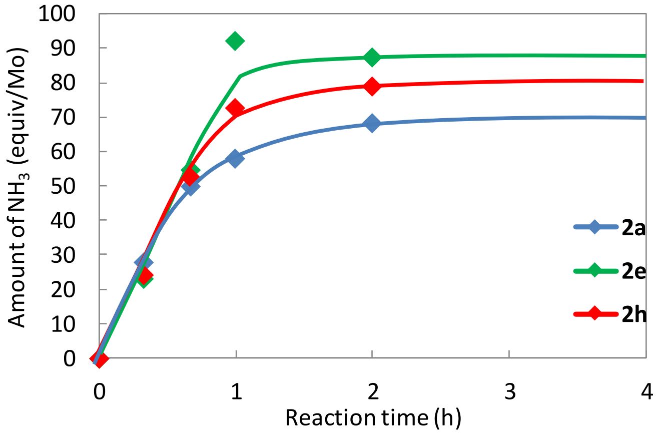

Fig. S1 Time profiles of ammonia formation with **2a** (blue), **2e** (green) and **2h** (red) as catalysts under slow addition of $CoCp^*_2$ conditions (0.72 mmol h^{-1}).

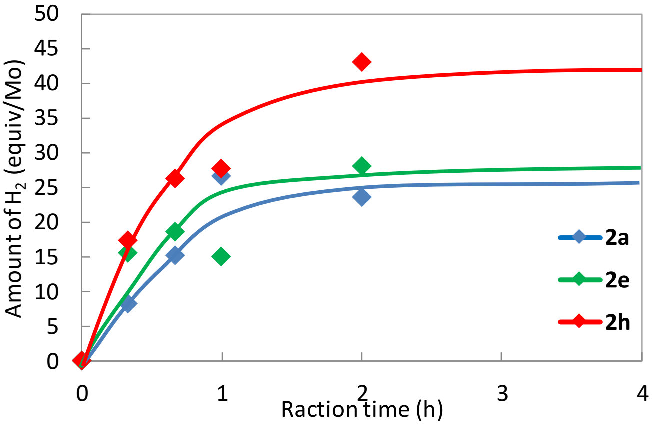

Fig. S2 Time profiles of molecular hydrogen formation with **2a** (blue), **2e** (green) and **2h** (red) as catalysts under slow addition of $CoCp^*_2$ conditions (0.72 mmol h^{-1}).

Table S1 The amounts of ammonia and dihydrogen catalyzed by **2a**

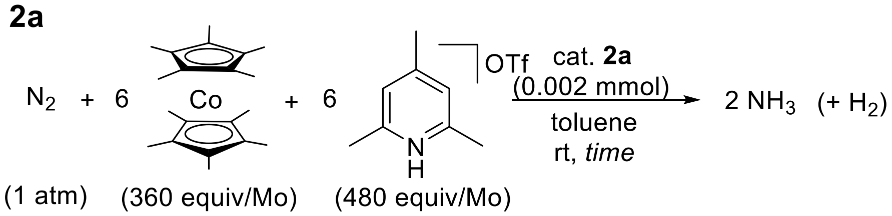

Entry	Time (h)	NH_3 (equiv)[a]	NH_3 (%)[b]	H_2 (equiv)[a]	H_2 (%)[b]
1	0.33	27.7	23	8.2	4.6
2	0.66	50	42	15.1	8.4
3	1	57.9	48	26.6	15
4	2	68.4	57	23.5	13
5	20	68.8	57	30.4	17

[a]Equiv based on the molybudenum atom. [b]Yield based on $CoCp^*_2$.

Table S2 The amounts of ammonia and dihydrogen catalyzed by **2e**

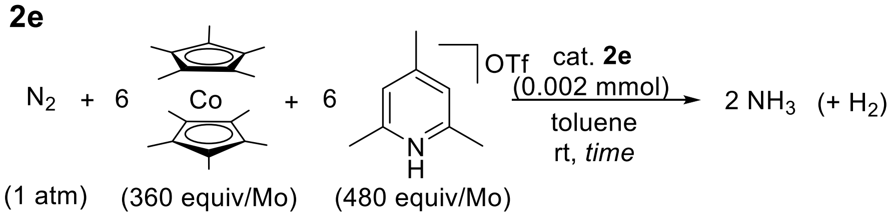

Entry	*time* (h)	NH_3 (equiv)[a]	NH_3 (%)[b]	H_2 (equiv)[a]	H_2 (%)[b]
1	0.33	22.9	19	15.6	8.7
2	0.66	54.6	46	18.6	10
3	1	92.3	77	15.0	8.3
4	2	87.4	73	28.1	16
5	20	90.4	75	27.3	15

[a]Equiv based on the molybudenum atom. [b]Yield based on $CoCp^*_2$.

Table S3 The amounts of ammonia and dihydrogen catalyzed by **2h**

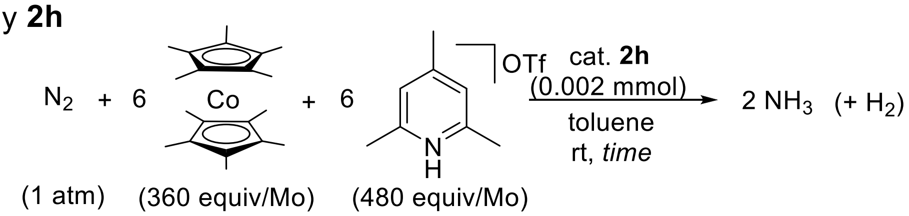

Entry	*time* (h)	NH_3 (equiv)[a]	NH_3 (%)[b]	H_2 (equiv)[a]	H_2 (%)[b]
1	0.33	24.0	20	17.4	9.7
2	0.66	52.4	44	26.2	15
3	1	72.7	61	27.6	15
4	2	78.8	66	43.0	24
5	20	82.6	70	42.2	23

[a] Equiv based on the molybudenum atom. [b] Yield based on CoCp*$_2$.

Time profiles of the formation of ammonia under one portion addition conditions.

A typical procedure is as follows. In a 50 mL Schlenk flask were placed CoCp$^*_2$ (180 equiv/Mo) and [ColH]OTf (240 equiv/Mo). A solution of **2a** (0.002 mmol) in toluene (5 mL) was added and stirred at room temperature. After the indicated time (0.5 min, 1 min, 2 min, and 5 min), a solution of potassium *tert*-butoxide (4.0 mmol) in THF (2 mL) was added to the reaction mixture to quench the reaction. The amount of molecular dihydrogen in the catalytic reaction was determined by GC analysis (5 min). Then 30wt% potassium hydroxide aqueous solution (5 mL) was added to the reaction mixture. The mixture was evaporated under reduced pressure, and the distillate was trapped in dilute H_2SO_4 solution (0.5 M, 10 mL). The amount of ammonia present in the H_2SO_4 solution was determined by the indophenol method.[S14] The results are summarized in Tables S4-S6.

Table S4 The amounts of ammonia and dihydrogen catalyzed by **2a**

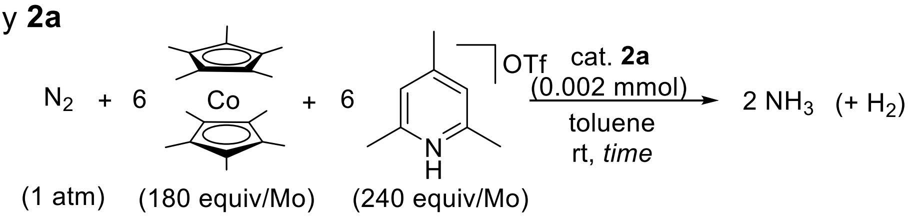

Entry	*time* (min)	NH_3 (equiv)[a]	NH_3 (%)[b]	H_2 (equiv)[a]	H_2 (%)[b]
1	0.5	3.5	5.8		
2	1	5.6	9.3		
3	2	8.9	15		
4	5	10.9	18	60.9	68

[a] Equiv based on the molybudenum atom. [b] Yield based on CoCp*$_2$.

Table S5 The amounts of ammonia and dihydrogen catalyzed by **2e**

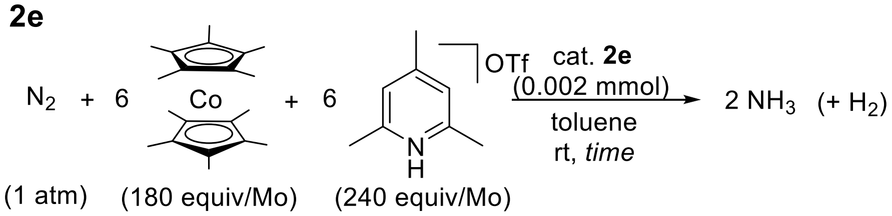

Entry	*time* (min)	NH_3 (equiv)[a]	NH_3 (%)[b]	H_2 (equiv)[a]	H_2 (%)[b]
1	0.5	8.1	14		
2	1	14.0	23		
3	2	15.7	26		
4	5	16.2	27	62.7	70

[a]Equiv based on the molybudenum atom. [b]Yield based on $CoCp^*_2$.

Table S6 The amounts of ammonia and dihydrogen catalyzed by **2h**

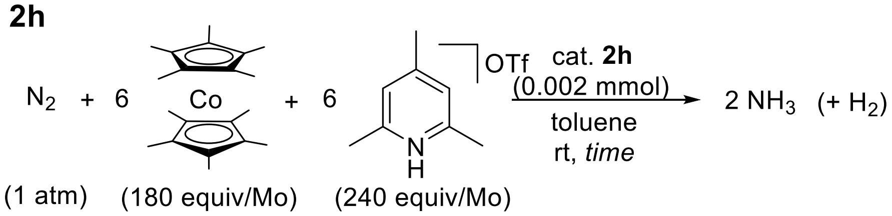

Entry	*time* (min)	NH_3 (equiv)[a]	NH_3 (%)[b]	H_2 (equiv)[a]	H_2 (%)[b]
1	0.5	6.2	10		
2	1	7.7	13		
3	2	10.8	18		
4	5	14.2	24	61.9	69

[a]Equiv based on the molybudenum atom. [b]Yield based on $CoCp^*_2$.

Stoichiometric Reduction of 2e and 2h·2THF with 2.2 equiv of $CoCp^*_2$ under N_2.

A typical procedure for the stoichiometric reduction of **2e** was described below. A mixture of **2e** (9.4 mg, 0.010 mmol) and $CoCp^*_2$ (7.2 mg, 0.022 mmol) in toluene (1 mL) was stirred at room temperature for 1 h under N_2 (1 atm). After volatiles were removed *in vacuo*, the residue was washed with pentane (1 mL x 3). The yields of [Mo(N)I(Ph-PNP$^{t\text{-Bu}}$)] (**3e**) in residual solid were determined by ^{1}H NMR in THF-d_8 using pentamethylbenzene as an internal standard (62% NMR yield).

Reaction of 3e and 3h·THF with $CoCp^*_2$ and [ColH]OTf under Ar.

A typical procedure for the stoichiometric reaction of **3e** with $CoCp^*_2$ and [ColH]OTf under Ar was described below. To a mixture of **3e** (14.2 mg, 0.0200 mmol), CoCp*2 (19.8 mg, 0.060 mmol, 3 equiv/Mo), and [ColH]OTf (21.8 mg, 0.080 mmol, 4 equiv/Mo) was added toluene (5 mL) under Ar atmosphere, and the mixture was stirred at room temperature for 2 h. Potassium hydroxide aqueous solution (30 wt%; 5 mL) was added to the reaction mixture. The mixture was evaporated under reduced pressure, and the distillate was trapped in dilute H_2SO_4 solution (0.5 M, 10 mL). The amount of ammonia was 0.0117 mmol (0.59 equiv/Mo, 59% yield) determined by the indophenol method.[S14]

X-ray crystallography.

Crystallographic data of **2c** (CCDC 1883301), **2d** (CCDC 1883302), **2e** (CCDC 1883303), **2f** (CCDC 1883304), **2g** (CCDC 1883305), **2h** (CCDC 1883306), **2i** (CCDC 1883307), **3e** (CCDC 1883308) and **3h**·THF (CCDC 1883309) are summarized in Tables S7–S9. ORTEP drawings with selected bond lengths and angles of these complexes are shown in Figs. S3–S11. Diffraction data were collected for 2 θ range of 4° to 55° at temperature ranging from – 92 to – 100 °C on a Rigaku RAXIS RAPID imaging plate area detector with graphite-monochromated Mo Kα radiation (λ = 0.71075 Å) with VariMax optics. Intensity data were corrected for Lorenz-polarization effects and for empirical absorption (ABSCOR). The structure solution and refinements were carried out by using the *CrystalStructure* crystallographic software package.[S16] The positions of the non-hydrogen atoms were determined by direct methods (SIR97[S17] for **2c**; SIR2011[S18] for **2d**; SHELXS Version 2013/1[S19] for **2e**, **2f**, **2g**, **2h**, and **3h**·THF; SIR92[S20] for **3e**) or heavy-atom Patterson methods (DIRDIF-PATTY[S21] for **2i**), and subsequent Fourier syntheses (SHELXL Version 2016/6[S22]), and were refined on F_o^2 using all unique reflections by full-matrix least-squares with anisotropic thermal parameters except for the disordered CH_2 and two ^{t}Bu groups bound to the P2 atom in **3e**, and the two disordered methyl groups and THF molecule in **3h**·THF.

For **3e**, the CH_2 (C7A vs C7B) and two ^{t}Bu groups (C22A–C23A–C24A–C25A vs C22B–C23B–C24B–C25B; C26A–C27A–C28A–C29A vs C26B–C27B–C28B–C29B) bound to the P2 atom were disordered among two positions in a ratio of 1:1, thus these non-hydrogen atoms were solved isotropically, and hydrogen atoms bound to these non-hydrogen atoms were not located. For **3h**·THF, two methyl groups (C28a vs C28b; C33a vs C33b) of the ^{t}Bu groups bound to the P2 atom were disordered among two positions in a ratio of 1:1, thus these non-hydrogen atoms were solved isotropically, and hydrogen atoms bound to these non-hydrogen atoms were not located. The THF molecule (O1–C34–C35–C36–C37) in **3h**·THF was also slightly disordered, thus these non-hydrogen atoms were solved isotropically, while hydrogen atoms bound to these carbon atoms were located at the calculated positions with isotropic parameters. All the other hydrogen atoms were placed at the calculated positions with fixed isotropic parameters. The unit cell of **2e**, **2h**, and **2i** contains solvent accessible voids of 4954, 1429, and 1518 Å^3, respectively. The difference Fourier maps suggested that voids of each crystals were occupied by two molar THF molecules per asymmetric unit, which could not be located appropriately because of heavy disorders. The electron density associated with these solvent molecules was removed by the SQUEEZE routine of PLATON[S22] for crystal data of **2e**, **2h**, and **2i**.

Table S7. X-ray crystallographic data for 2c, 2d, 2e.

	2c	**2d**	**2e**
chemical formula	$C_{19}H_{35}I_3MoNP_2$	$C_{31}H_{27}I_3MoNP_2$	$C_{37}H_{71}I_5Mo_2N_2P_5$
CCDC number	1883301	1883302	1883303
formula weight	816.09	952.16	1463.31
dimensions of crystals, mm^3	0.30 × 0.10 × 0.10	0.15 × 0.06 × 0.01	0.25 × 0.10 × 0.05
crystal color, habit	orange, platelet	orange, platelet	red, block
crystal system	Orthorhombic	Triclinic	monoclinic
space group	*Pbca*	$P\bar{1}$	*I*2/*a*
a, Å	26.9513(9)	10.8646(7)	24.7398(5)
b, Å	17.2697(6)	11.4437(7)	25.2842(5)
c, Å	11.1949(3)	13.9846(10)	25.498(3)
α, deg	90	96.216(7)	90
β, deg	90	98.933(7)	118.700(5)
γ, deg	90	109.654(8)	90
V, Å^3	5210.6(3)	1593.3(2)	13990.2(19)
Z	8	2	16
ρ_{calcd}, g cm^{-3}	2.080	1.985	2.779
$F(000)$	3096	902	11216
μ, cm^{-1}	41.875	34.402	53.059
temperature, °C	–100	–100	–100
trans. factors range	0.434 – 0.658	0.392 – 0.966	0.504 – 0.767
no. reflections measured	47008	15057	66785
no. unique reflections	5967 (R_{int} = 0.1510)	7129 (R_{int} = 0.0593)	15990 (R_{int} = 0.0589)
no. parameters refined	243	343	508
$R1$ ($I > 2\sigma(I)$)[a]	0.0720	0.0699	0.0488
$wR2$ (all data)[b]	0.1763	0.1928	0.1085
GOF (all data)[c]	1.000	1.101	1.026
max diff peak / hole, e Å^{-3}	+2.28 / –1.97	+1.92 / –2.16	+1.41 / –1.29

[a] $R1 = \Sigma||F_o|-|F_c||/\Sigma|F_o|$. [b] $wR2 = [\Sigma w(F_o^2-F_c^2)^2/\Sigma w(F_o^2)^2]^{1/2}$, $w = 1/[\sigma^2(F_o^2) + (qP)^2 + rP]$, $P = (\mathrm{Max}(F_o^2, 0) + 2F_c^2)/3$ [q = 0 (**2c**), 0.1 (**2d**), 0.0511 (**2e**); r = 235 (**2c**), 0 (**2d**), 32.1426 (**2e**)]. [c] GOF = $[\Sigma w(F_o^2-F_c^2)^2/(N_o-N_{\mathrm{params}})]^{1/2}$.

Table S8. X-ray crystallographic data for 2f, 2g, 2h.

	2f	**2g**	**2h**
chemical formula	$C_{24}H_{45}I_3MoNP_2$	$C_{24}H_{45}I_3MoNOP_2$	$C_{33}H_{51}FeI_3MoNP_2$
CCDC number	1883304	1883305	1883306
formula weight	886.23	902.23	1056.22
dimensions of crystals, mm^3	0.06 × 0.04 × 0.01	0.10 × 0.10 × 0.05	0.35 × 0.25 × 0.20
crystal color, habit	red, block	brown, block	red, block
crystal system	Tetragonal	tetragonal	monoclinic
space group	$I4_1/a$	$I4_1/a$	$P2_1/n$
a, Å	23.5322(6)	23.7105(10)	14.8370(5)
b, Å	23.5322(6)	23.7105(10)	18.7561(5)
c, Å	21.9910(6)	22.0142(5)	17.0679(5)
α, deg	90	90	90
β, deg	90	90	90.450(6)
γ, deg	90	90	90
V, $Å^3$	12177.8(6)	12376.1(8)	4749.6(2)
Z	16	16	4
ρ_{calcd}, g cm^{-3}	1.933	1.937	1.477
$F(000)$	6832	6960	2052
μ, cm^{-1}	35.918	35.384	26.050
temperature, °C	–100	–100	–100
trans. factors range	0.784 – 1.000	0.579 – 0.838	0.326 – 0.594
no. reflections measured	57843	57855	44979
no. unique reflections	6871 (R_{int} = 0.1248)	6870 (R_{int} = 0.1161)	10887 (R_{int} = 0.0481)
no. parameters refined	293	302	382
$R1$ ($I > 2\sigma(I)$)^a	0.0552	0.0692	0.0486
$wR2$ (all data)^b	0.1502	0.1652	0.1062
GOF (all data)^c	0.987	1.074	1.071
max diff peak / hole, e $Å^{-3}$	+1.90 / –2.74	+1.99 / –2.54	+1.05 / –1.27

[a] $R1 = \Sigma||F_o|-|F_c||/\Sigma|F_o|$. [b] $wR2 = [\Sigma w(F_o^2-F_c^2)^2/\Sigma w(F_o^2)^2]^{1/2}$, $w = 1/[\sigma^2(F_o^2) + (qP)^2 + rP]$, $P = (\mathrm{Max}(F_o^2, 0) + 2F_c^2)/3$ [q = 0.0865 (**2f**) 0.0785 (**2g**) 0.0383 (**2h**); r = 13.3585 (**2f**), 153.1422 (**2g**), 13.3413 (**2h**)]. [c] GOF = $[\Sigma w(F_o^2-F_c^2)^2/(N_o-N_{params})]^{1/2}$.

Table S9. X-ray crystallographic data for 2i, 3e, 3h·THF.

	2i	**3e**	**3h**·THF
chemical formula	$C_{33}H_{51}I_3MoNP_2Ru$	$C_{29}H_{47}IMoN_2P_2$	$C_{37}H_{59}FeIMoN_2OP_2$
CCDC number	1883307	1883308	1883309
formula weight	1101.44	708.50	888.52
dimensions of crystals, mm^3	0.15 × 0.10 × 0.02	0.15 × 0.10 × 0.10	0.10 × 0.10 × 0.05
crystal color, habit	brown, platelet	brown, block	red, block
crystal system	Monoclinic	monoclinic	monoclinic
space group	$P2_1/n$	$C2/c$	Cc
a, Å	15.0489(6)	19.962(2)	21.9017(10)
b, Å	18.7575(7)	18.924(2)	15.3078(8)
c, Å	17.1035(8)	18.744(2)	13.8750(6)
α, deg	90	90	90
β, deg	90.845(6)	114.643(8)	120.601(9)
γ, deg	90	90	90
V, Å^3	4827.4(4)	6435.9(13)	4004.0(5)
Z	4	8	4
ρ_{calcd}, g cm^{-3}	1.515	1.462	1.474
F(000)	2124	2880	1816
μ, cm^{-1}	25.758	14.854	15.552
temperature, °C	–100	–92	–100
trans. factors range	0.673 – 0.950	0.395 – 0.862	0.642 – 0.925
no. reflections measured	45553	27943	17366
no. unique reflections	10995 (R_{int} = 0.1312)	6907 (R_{int} = 0.0989)	8373 (R_{int} = 0.0380)
no. parameters refined	382	313	409
$R1$ ($I > 2\sigma(I)$)^a	0.0896	0.1377	0.0725
$wR2$ (all data)^b	0.2591	0.2433	0.1313
GOF (all data)^c	1.009	1.000	1.004
max diff peak / hole, e Å^{-3}	+3.58 / –1.13	+2.38 / –1.35	+2.49 / –1.15
Flack parameter			0.019(11)

[a] $R1 = \Sigma||F_o|-|F_c||/\Sigma|F_o|$. [b] $wR2 = [\Sigma w(F_o^2-F_c^2)^2/\Sigma w(F_o^2)^2]^{1/2}$, $w = 1/[\sigma^2(F_o^2) + (qP)^2 + rP]$, $P = (\mathrm{Max}(F_o^2, 0) + 2F_c^2)/3$ [q = 0.1387 (**2i**), 0 (**3e**), 55 (**3h**·C_4H_8O); r = 0 (**2i**, **3h**·C_4H_8O), 367 (**3e**)]. [c] GOF = $[\Sigma w(F_o^2-F_c^2)^2/(N_o-N_{\mathrm{params}})]^{1/2}$.

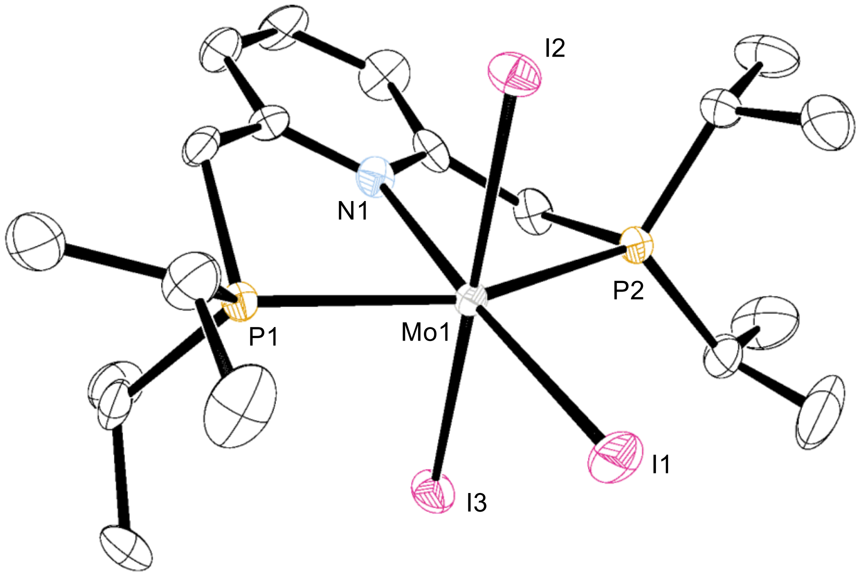

Fig. S3 Molecular structure of [MoI$_3$(H-PNP$^{i\text{-Pr}}$)] (**2c**). Thermal ellipsoids are shown at the 50% probability level, and hydrogen atoms are omitted for clarity. Selected bond lengths (Å) and angles (deg):Mo1–N1 2.231(8), Mo1–P1 2.556(3), Mo1–P2 2.556(3), Mo1–I1 2.7475(11), Mo1–I2 2.7623(11), Mo1–I3 2.7760(11); P1–Mo1–P2 156.81(9).

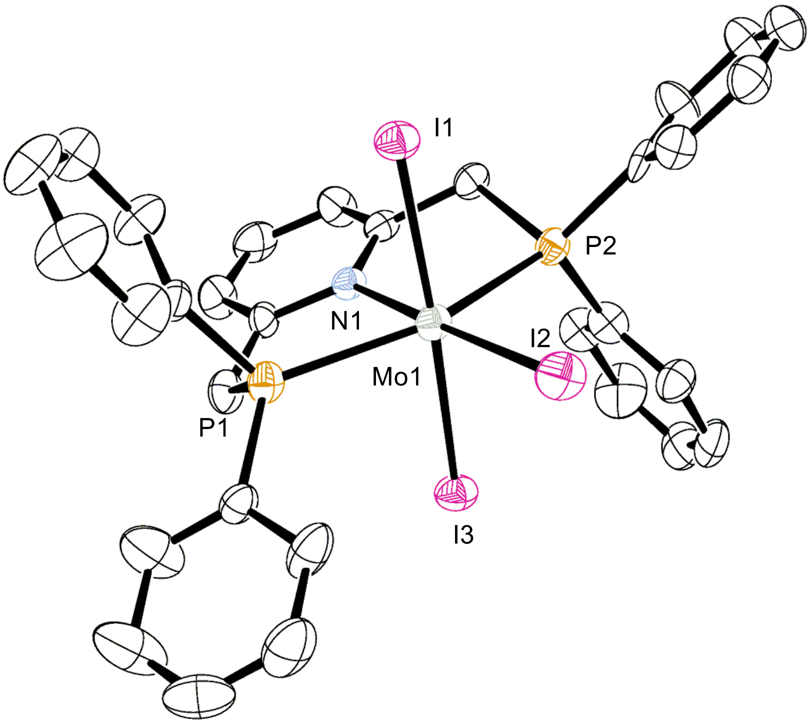

Fig. S4 Molecular structure of [MoI$_3$(H-PNP$^{\text{Ph}}$)] (**2d**). Thermal ellipsoids are shown at the 50% probability level, and hydrogen atoms are omitted for clarity. Selected bond lengths (Å) and angles (deg): Mo1–N1 2.238(7), Mo1–P1 2.538(3), Mo1–P2 2.511(3), Mo1–I1 2.7365(11), Mo1–I2 2.7058(10), Mo1–I3 2.7545(11); P1–Mo1–P2 157.08(9).

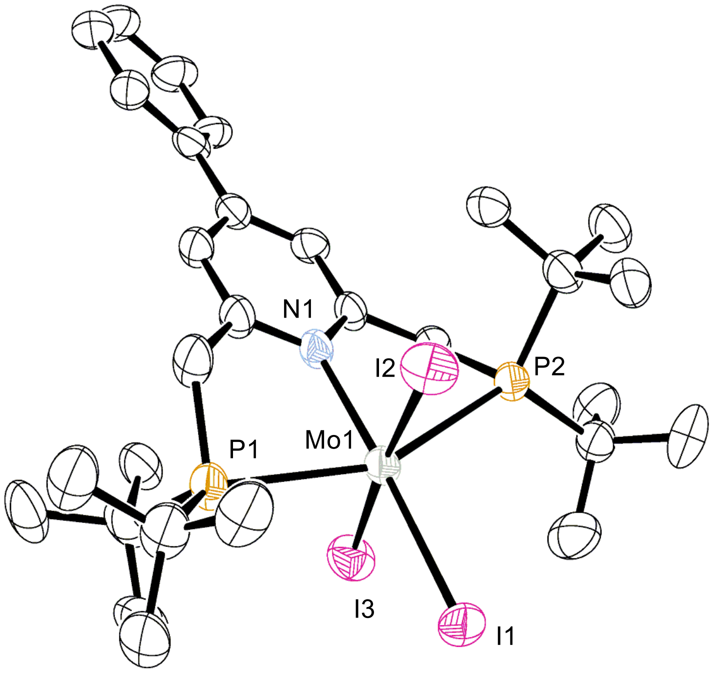

Fig. S5 Molecular structure of one of the one and a half crystallographically independent molecules of [$\mathrm{MoI_3}$(Ph-PNP$^{t\text{-Bu}}$)] (**2e**). Thermal ellipsoids are shown at the 50% probability level, and hydrogen atoms are omitted for clarity. Selected bond lengths (Å) and angles (deg): Mo1–N1 2.202(4), Mo1–N2 2.180(5), Mo1–P1 2.6576(14), Mo1–P2 2.6689(12), Mo1–P3 2.6956(12), Mo1–P3* 2.6957(11) Mo1–I1 2.7576(5), Mo1–I2 2.7970(6), Mo1–I3 2.7695(6), Mo2–I4 2.7473(7), Mo2–I5 2.7823(3); P1–Mo1–P2 153.52(4), P3–Mo2–P3* 155.01(5).

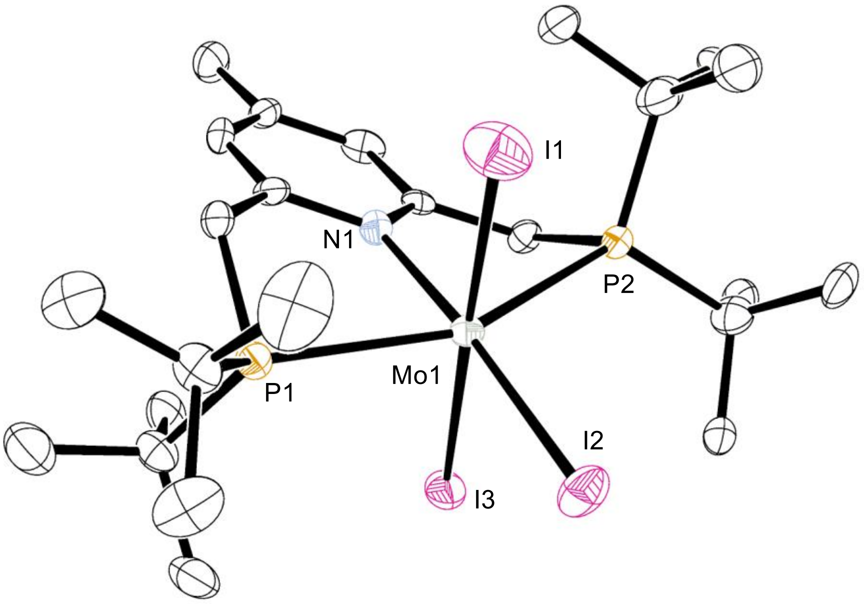

Fig. S6 Molecular structure of [$\mathrm{MoI_3}$(Me-PNP$^{t\text{-Bu}}$)] (**2f**). Thermal ellipsoids are shown at the 50% probability level, and hydrogen atoms are omitted for clarity. Selected bond lengths (Å) and angles (deg):Mo1–N1 2.197(6), Mo1–P1 2.650(2), Mo1–P2 2.6544(19), Mo1–I1 2.7232(9), Mo1–I2 2.7610(8), Mo1–I3 2.8381(8); P1–Mo1–P2 155.17(6).

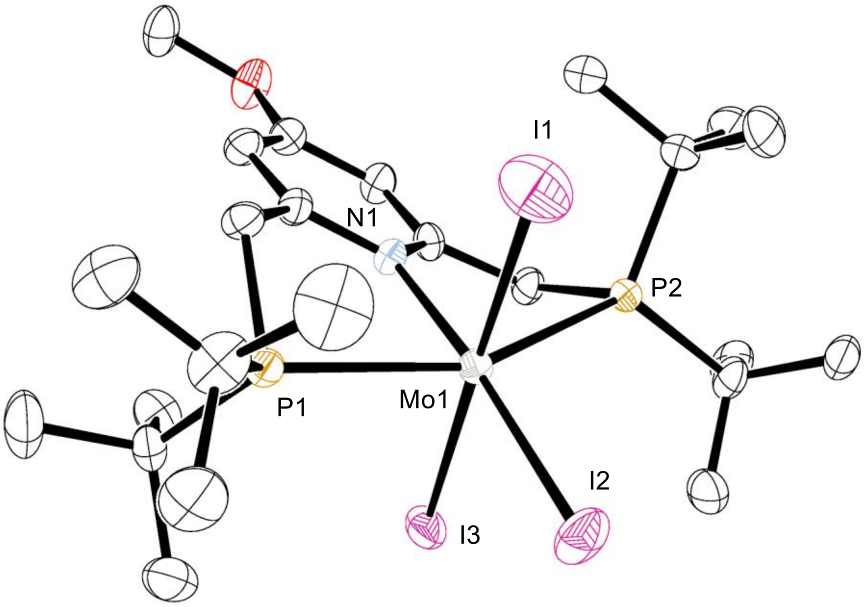

Fig. S7 Molecular structure of [MoI$_3$(MeO-PNP$^{t\text{-Bu}}$)] (**2g**). Thermal ellipsoids are shown at the 50% probability level, and hydrogen atoms are omitted for clarity. Selected bond lengths (Å) and angles (deg):Mo1–N1 2.174(7), Mo1–P1 2.648(2), Mo1–P2 2.658(2), Mo1–I1 2.7168(11), Mo1–I2 2.7594(9), Mo1–I3 2.8519(9); P1–Mo1–P2 154.30(7).

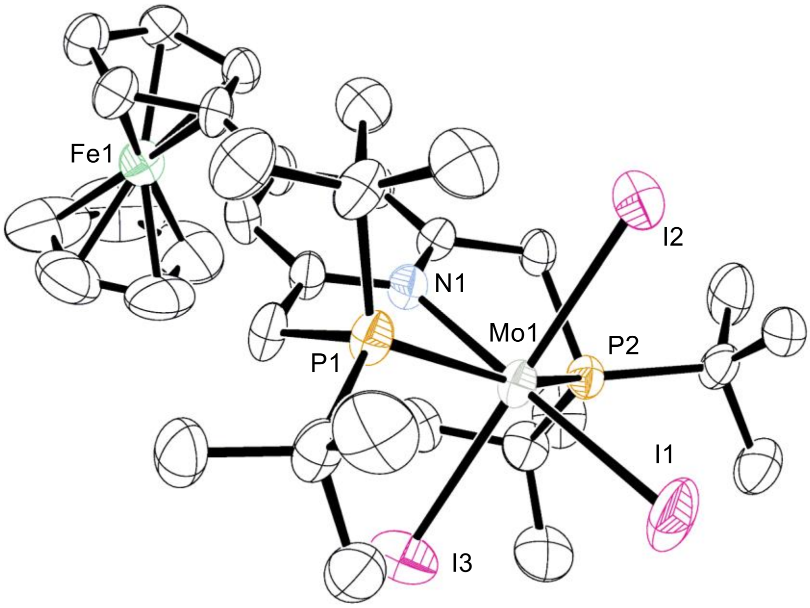

Fig. S8 Molecular structure of [MoI$_3$(Fc-PNP$^{t\text{-Bu}}$)] (**2h**). Thermal ellipsoids are shown at the 50% probability level, and hydrogen atoms are omitted for clarity. Selected bond lengths (Å) and angles (deg):Mo1–N1 2.185(3), Mo1–P1 2.6501(12), Mo1–P2 2.6588(12), Mo1–I1 2.7491(5), Mo1–I2 2.7963(5), Mo1–I3 2.7605(5); P1–Mo1–P2 154.54(4).

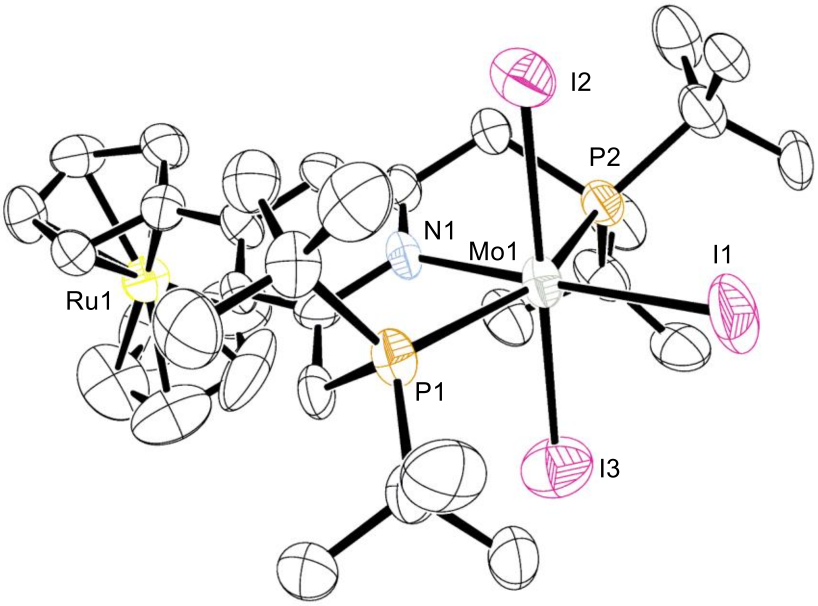

Fig. S9 Molecular structure of [MoI$_3$(Rc-PNP$^{t\text{-Bu}}$)] (**2h**). Thermal ellipsoids are shown at the 50% probability level, and hydrogen atoms are omitted for clarity. Selected bond lengths (Å) and angles (deg):Mo1–N1 2.187(8), Mo1–P1 2.636(3), Mo1–P2 2.644(3), Mo1–I1 2.7413(12), Mo1–I2 2.8234(12), Mo1–I3 2.7522(13); P1–Mo1–P2 154.54(4).

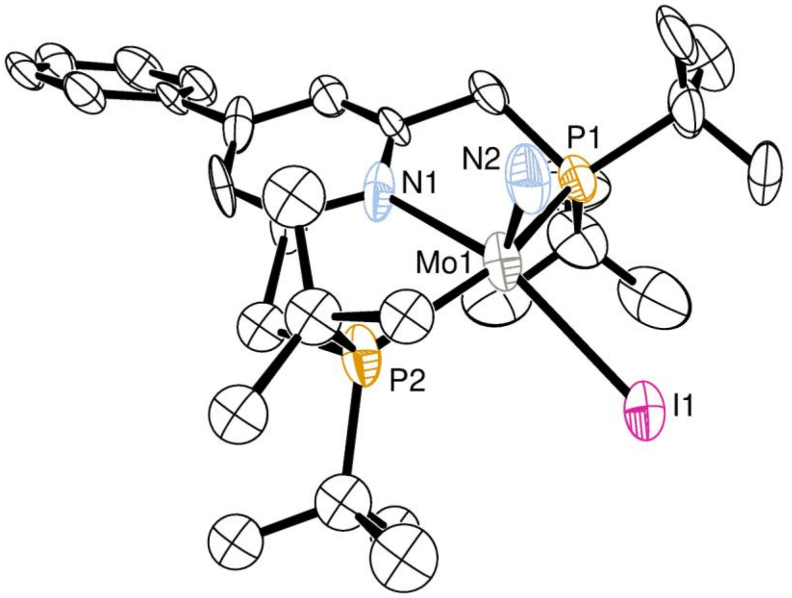

Fig. S10 Molecular structure of [Mo(N)I(Ph-PNP$^{t\text{-Bu}}$)] (**3e**). Thermal ellipsoids are shown at the 50% probability level, and ones of the two disorders of the CH$_2$ and two ^{t}Bu groups bound to the P2 atom as well as hydrogen atoms are omitted for clarity. Selected bond lengths (Å) and angles (deg):Mo1–N1 2.258(10), Mo1–N2 1.672(14), Mo1–P1 2.480(4), Mo1–P2 2.508(4), Mo1–I1 2.8451(16); P1–Mo1–P2 153.31(12), N1–Mo1–I1 155.5(3), N2–Mo1–I1 104.2(4), N1–Mo1–N2 100.3(5).

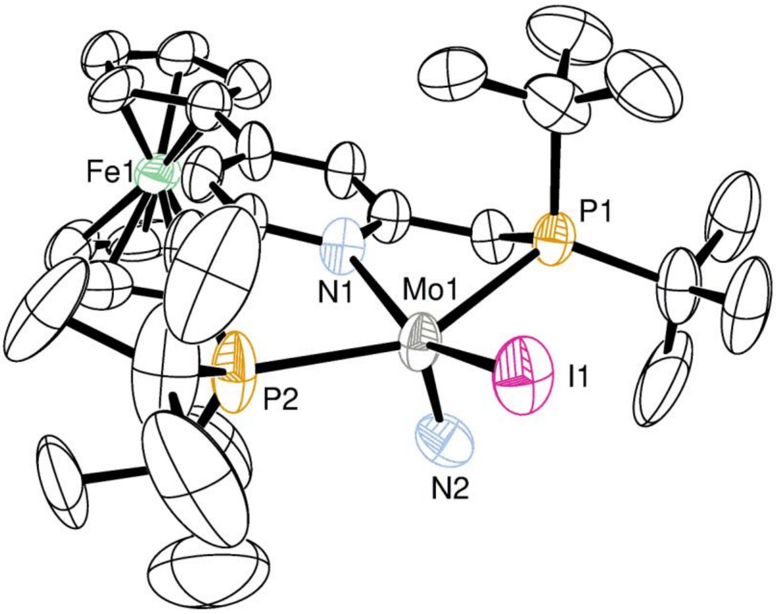

Fig. S11 Molecular structure of [Mo(N)I(Fc-PNP$^{t\text{-Bu}}$)] (**3h**). Thermal ellipsoids are shown at the 50% probability level, and ones of the two disordered methyl groups as well as THF molecule are omitted for clarity. Selected bond lengths (Å) and angles (deg):Mo1–N1 2.211(10), Mo1–N2 1.649(11), Mo1–P1 2.479(4), Mo1–P2 2.504(4), Mo1–I1 2.8217(13); P1–Mo1–P2 151.94(14), N1–Mo1–I1 150.1(3), N2–Mo1–I1 107.1(4), N1–Mo1–N2 102.4(5).

References.

S1. G. A. Bain and J. F. Berry, *J. Chem. Educ*. 2008, **85**, 532.

S2. M. Kawatsura and J. F. Hartwig, *Organometallics,* 2011, **20**, 1960.

S3. H. Neumann, A. Sergeev and M. Beller, *Angew. Chem., Int. Ed.*, 2008, **47**, 4887.

S4. W. P. Leung, Q. W. Y. Ip, S. Y. Wong and T. C. W. Mak, *Organometallics*, 2003, **22**, 4604.

S5. C. M. Brian and M. E. Forrest, *J. Am. Chem. Soc.*, 2008, **130**, 2786.

S6. S. Kuriyaka, K. Arashiba, K. Nakajima, H. Tanaka, N. Kamaru, K. Yoshizawa and Y. Nishibayashi, *J. Am. Chem. Soc.*, 2014, **136**, 9719.

S7. S. Kuriyama, K. Arashiba, K. Nakajima, H. Tanaka, K. Yoshizawa and Y. Nishibayashi, *Chem. Sci.*, 2015, **6**, 3940.

S8. F. Stoffelbach, D. Saurenz and R. Poli, *Eur. J. Inorg. Chem*., 2001, 2699.

S9. R. Poli, S. T. Krueger and S. P. Mattamana, *Inorg. Synth.,* 1998, **32**, 198.

S10. K. Arashiba , A. Eizawa, H. Tanaka, K. Nakajima, K. Yoshizawa and Y. Nishibayashi, *Bull. Chem. Soc. Jpn.*, 2017, **90**, 1111.

S11. K. Arashiba, E. Kinoshita, S. Kuriyama, A. Eizawa, K. Nakajima, H. Tanaka, K. Yoshizawa and Y. Nishibayashi, *J. Am. Chem. Soc*., 2015, **137**, 5666.

S12. D. V. Yandulov and R. R. Schrock, *Can. J. Chem.,* 2005, **83**, 341.

S13. I. S. Weitz and M. Rabinovitz, *J. Chem. Soc.*, *Perkin Trans.*, 1993, **1**, 117.

S14. M. W. Weatherburn, *Anal. Chem.*, 1967, **39**, 971.

S15. G. W. Watt and J. D. Chrisp, *Anal. Chem.*, 1952, **24**, 2006.

S16. CrystalStructure 4.3: Crystal Structure Analysis Package, Rigaku Corporation, Tokyo, Japan, 2018.

S17. A. Altomare, M. C. Burla, M. Camalli, G. L. Cascarano, C. Giacovazzo, A. Guagliardi, A. G. G. Moliterni, G. Polidorib and R. Spagna, *J. Appl. Crystallogr.,* 1999, **32**, 115.

S18. M. C. Burla, R. Caliandro, M. Camalli, B. Carrozzini, G. L. Cascarano, C. Giacovazzo, M. Mallamo, A. Mazzone, G. Polidori and R. Spagna, *J. Appl. Crystallogr.,* 2012, **45**, 357.

S19. G. M. Sheldrick, *Aca Crystallogr.,* 2008, **A64**, 112.

S20 A. Altomare, G. Cascarano, C. Giacovazzo and A. Guagliardi, *J. Appl. Crystallogr.,* 1993, **26**, 343.

S21. P. T. Beurskens, G. Admiraal, H. Behm, G. Beurskens, W. P. Bosman, S. García-Granda, R. O. Gould, J. M. M. Smits and C. Smykalla, *Z. Kristallogr., Suppl.,* 1991, **4**, 99.

S22. G. M. Sheldrick, *Acta Crystallogr.,* 2015, **C71**, 3.

S23. A. L. Spek, *Acta Crystallogr.,* 2015, **C71**, 9.